Published in final edited form as:
J Magn Reson Imaging. 2010 February ; 31(2): 406–415. doi:10.1002/jmri.22043.

MRI Measurements of Carotid Plaque in the Atherosclerosis Risk in Communities (ARIC) Study: Methods, Reliability and Descriptive Statistics

Bruce A. Wasserman, MD[1,*], **Brad C. Astor, PhD, MPH**[2,3], **A. Richey Sharrett, MD, DrPH**[2], **Cory Swingen, PhD**[4], and **Diane Catellier, PhD**[5]

[1]The Russell H. Morgan Department of Radiology and Radiological Sciences, The Johns Hopkins University School of Medicine, Baltimore, Maryland, USA

[2]Department of Epidemiology, The Johns Hopkins Bloomberg School of Public Health, Baltimore, Maryland, USA

[3]Department of Medicine, The Johns Hopkins University School of Medicine, Baltimore, Maryland, USA

[4]Department of Medicine, University of Minnesota Medical School, Minneapolis, Minnesota, USA

[5]Department of Statistics, University of North Carolina School of Public Health, Chapel Hill, North Carolina, USA

Abstract

Purpose—To measure carotid plaque components using MRI and estimate reliability in the population-based Atherosclerosis Risk in Communities (ARIC) study.

Materials and Methods—Contrast-enhanced high-resolution ($0.51 \times 0.58 \times 2$ mm^3) MRI images were acquired through internal (ICA) and common carotid arteries (CCA) of 2066 ARIC participants at four sites. Sixty-one exams were repeated and 164 pairs had repeated interpretations. Plaque component thicknesses, areas and volumes over eight slices (1.6-cm segment) were measured. Intraplaque hemorrhage was recorded. Reliability was evaluated by intraclass correlations and κ statistics.

Results—There were 1769 successful MRI exams (mean age 71 years; 57% females; 81% white; 19% African-Americans). Repeat scan reliability was highest for CCA lumen area (0.94) and maximum wall thickness (0.89), ICA lumen area (0.89) and maximum wall thickness (0.77) and total wall volume (0.79), and lowest for small structures—core volume (0.30) and mean cap thickness (0.38). Overall reliability was primarily related to reader variability rather than scan acquisition. K's for presence of core, calcification and hemorrhage were fair to good. White men had the thickest plaques (average maximum ICA wall thickness = 2.3 mm) and the most cores (34%).

Conclusion—The most important limiting factor for MRI measurements of plaque components is reader variability. Measurement error depends largely on the analyzed structure's size.

Keywords

atherosclerosis; epidemiology; magnetic resonance imaging; plaque; statistics

[*]Address reprint requests to: B.A.W., The Johns Hopkins Hospital, 367 East Park Building, 600 N. Wolfe Street, Baltimore, MD 21287. bwasser@jhmi.edu .

Development, progression and clinical manifestations of cardiovascular disease are related to specific pathologic characteristics of the arterial wall. The advent of high-resolution MRI has enabled the investigation of such characteristics in large populations because of its ability to reveal atherosclerotic plaque components noninvasively (1,2). In particular, in vivo MRI studies have demonstrated the ability to discriminate the lipid core, fibrous cap, calcification, and intraplaque hemorrhage (3). Wall area and plaque burden also can be accurately measured by suppressing the signal of flowing blood in the lumen using black blood MR techniques (4). A double inversion-recovery (DIR) sequence (5) is commonly used for this purpose. The administration of a gadolinium contrast agent during MRI improves the discrimination of plaque components, enabling its more reliable characterization (6–8), and improves the measurements of wall volume and area (9). Both DIR and quadruple inversion-recovery techniques have been used successfully to suppress flow following contrast admin-istration (7,10,11).

The Atherosclerosis Risk in Communities (ARIC) Carotid MRI study, described herein, enrolled 2066 community-representative men and women, aged 65 to 84 years to investigate the genomic, metabolic and cellular correlates of carotid plaque components. The purpose of this study was to measure carotid wall and plaque dimensions and determine plaque component prevalence representative of the general population using MRI, and estimate the reliability of these measurements.

MATERIALS AND METHODS

Study Design and Study Participants

ARIC was initiated in 1987 to study cardiovascular diseases in African-American and white men and women (N = 15,792), ages 45 to 64 years, selected to represent four US communities (Forsyth County, NC; Jackson, MS; suburban Minneapolis, MN; and Washington County, MD, USA) (12). Four examinations since 1987 provided an extensive database of predictors of atherosclerosis and its clinical sequelae.

For the current study, ARIC participants were selected using a stratified plan to oversample for plaque based on carotid thickness at a prior ultrasound examination (1993–1998). Carotid intima-media thickness (IMT) cutpoints were selected to recruit approximately 1200 with thick walls and 800 from the remainder. The cutpoints ranged from 1.00 mm to 1.28 mm (69th to 73rd percentile) across centers to allow for an approximately equal distribution of participants across field centers.

Participants with contraindications to MRI or contrast media were excluded, as were those who could not provide informed consent. Participants who had a prior carotid endarterectomy on either side (for the group below the IMT cutpoint) or on the side selected for imaging (for the group above the cutpoint) also were excluded.

A total of 4306 persons were invited: 1403 refused, 837 were ineligible, and 2066 participated. Institutional review boards of the four centers approved this HIPAA-compliant study, and written informed consent was obtained from all participants.

Over the course of the study, 61 randomly selected participants repeated the entire clinic visit including the MRI exam within four to eight weeks to estimate total MRI measurement error from both scan acquisition and reader variability. Within-person biologic variation was not expected to be an important source of variability because of the short between-scan intervals. These participants were assigned alternate IDs to ensure blinding of both the MRI technologists and the readers.

Reader reliability was estimated by randomly reassigning some scans for interpretation by the same ($N = 53$) or different ($N = 111$) reader. Exam IDs were changed and readers were unaware these were repeated interpretations. The target interval between readings by the same analyst was at least 90 days to minimize the influence of recall. Participants with lipid cores were oversampled for repeat readings.

MRI Protocol

A standard MRI protocol was used for all participants and performed on 1.5T scanners (Excite platform, GE Medical Systems, Forsyth County, Jackson, and Washington County, USA; Symphony Maestro, Siemens Medical Solutions, Minneapolis, USA) using bilateral four-element phased array carotid coils (Machnet, The Netherlands). Fourteen MRI technologists, trained centrally and certified by the MRI Reading Center, acquired the scans. Total protocol time was less than one hour.

A 3D time-of-flight (TOF) MR angiogram (MRA) was acquired through both carotid bifurcations (acquired resolution = $0.59 \times 0.59 \times 2$ mm^3). Black blood MRI (BBMRI) images were then acquired using a 2D electrocardiogram (ECG)-gated DIR fast spin-echo sequence based on a standardized protocol (2,7) as follows: slice thickness = 2 mm; field-of-view = 13 cm; matrix = 256 × 224; echo-train-length = 10; 1 signal average; acquired resolution = $0.51 \times 0.58 \times 2$ mm^3. Three long-axis BBMRI slices were acquired through each carotid bifurcation using the MRA as a scout image (repetition time/echo time/inversion time = 2 RR/5 msec/600 msec). The BBMRI image best depicting each bifurcation and flow divider (FD) was used to orient transverse BBMRI images, acquired using chemical suppression of fat signal and the following parameters: repetition time/echo time = 1 RR/ 5 msec, inversion time = 350 msec. A single transverse T1-weighted BBMRI slice was acquired through each distal common carotid artery (CCA), positioned 1.5 cm below the FD and oriented perpendicular to the vessel axis (Fig. 1). Eight transverse T1-weighted BBMRI images (longitudinal coverage = 1.6 cm) were then acquired through the carotid bifurcation found to have the greater maximum wall thickness at the participant's most recent ultrasound scan (Fig. 2a) or through the contralateral carotid if its wall appeared thicker on the MRA source images or more stenotic on the MRA maximum intensity projection (MIP) images to the MRI technologist. The slices were centered at the thickest part of the carotid wall, or at the FD if no wall thickening was observed. Slices were parallel and oriented perpendicular to the overall vessel axis or plaque, if present.

A 3D contrast-enhanced MRA was acquired during the intravenous injection of gadodiamide (Omniscan, GE Healthcare), 0.1 mmol/kg, by power injector. Transverse T1-weighted BBMRI slices were acquired beginning five minutes after contrast injection with the same MRI parameters used for the precontrast acquisitions except the inversion time was adjusted to account for contrast (200 msec). First, transverse slices through each distal CCA were repeated, and then 16 transverse slices (longitudinal coverage = 3.2 cm) were acquired through the previously-imaged carotid bifurcation. For slice positioning, the eight precontrast transverse slices were copied with three slices added below and five slices added above.

Image Analysis

Seven readers were certified to interpret the MRI images using semiautomated software (VesselMASS, Leiden University Medical Center), following a minimum three month training period. The readers were blinded to participant characteristics. All exams were assigned quality control (QC) scores (0 to 2) that graded image quality and protocol adherence. Failed exams (score = 0) were not analyzed. Only the eight slices with matching precontrast and postcontrast images were analyzed. If the postcontrast slices showing the thickest wall and FD were not included, the reader continued analyzing to include these slices and all slices in-between. The CCA precontrast and post-contrast image pairs also were analyzed.

Contours were drawn on the postcontrast series to delineate the lipid core, calcification, and outer wall (Fig. 2). Postcontrast images were used for plaque component measurements because gadolinium administration improves discrimination of plaque features (7,8). Calcification was distinguished from ulceration using the TOF MRA source image (calcification identified as dark, ulceration as bright). The lumen contours were drawn on precontrast images to minimize flow artifacts exaggerated by gadolinium contrast and copied onto postcontrast images with adjustment for wall motion. Multiplanar reconstructions of the contrast-enhanced MRA source images were also used to confirm lumen contours on black blood images. The fibrous cap contour was automatically generated based on lipid core and lumen contours. Intraplaque hemorrhage was identified using established criteria (hyperintense on precontrast T1-weighted BBMRI and TOF MRA images (13)) by one reader.

The semiautomated analysis software divided vessel walls into 12 radial segments and fibrous caps into radial segments at 15° increments for each slice (Fig. 2e). Thickness and signal intensity (SI) values were generated for each segment. Area and SI measurements were generated for lipid core and calcification contours. Volumetric data were computed by integrating area measurements over eight contiguous slices, selected to include the thickest wall, covering 1.6 cm.

Percent stenosis was measured for each carotid artery using North American Symptomatic Carotid Endarterectomy Trial (NASCET) criteria (14) based on the TOF MRA MIP images, unless poor image quality precluded interpretation (143 participants, 7%), in which case the contrast-enhanced MRA MIPs were used. Participants were notified by letter if stenosis ≥50% was detected.

Statistical Methods

Distributions of MRI variables were described separately for race and sex groups using means, standard deviations, and percentiles. Sampling weights were used in these analyses to account for the oversampling of thick carotids and provide estimates referable to the overall ARIC population. Standard errors were estimated using a robust variance estimator, taking into account correlation within sampling groups, using SAS version 9.1 (SAS Institute Inc, NC, USA). Tests of equality of means and proportions across race and sex groups were based on an analysis of variance (ANOVA) using SUDAAN software, version 9.0.1 (RTI, NC, USA) and the Rao-Scott chi-squared test from the surverfreq procedure, respectively. Reliability of continuous MRI variables was estimated by intra-class correlations under a random effects model (15). The average within-person standard deviations are provided.

For dichotomous measures we used percent agreement and κ statistics (16). Reliabilities and κ statistics below 0.4 were characterized as poor agreement, 0.4 to 0.75 as fair to good, and above 0.75 as excellent (16). Reliability was estimated for the entire sample and for subpopulations grouped by precontrast SI of the wall to confirm that signal loss due to deeper vessels did not introduce greater measurement error. Precontrast images were used so that wall signal was primarily dependent on vessel depth and not influenced by vessel wall enhancement.

RESULTS

Of the 2066 ARIC members who participated in the Carotid MRI substudy, 1938 completed an MRI examination. Reasons for 128 (6%) incomplete MRI exams included: 4% = determined to be ineligible at the time of the scan; 6% = unable to lie in the scanner; 11% = scan aborted/incomplete; 30% = refused participation (e.g., claustrophobia); 50% = unknown. Of the 1938 with completed scans, attributes could not be ascertained for 169 (i.e., for the CCA [*N* = 18, 11%], internal carotid arteries [ICA, *N* = 87, 51%], or both [*N* = 64, 38%]) because of either protocol deviations or poor image quality. All analyses were based on the remaining 1769 scans

(ages 60–84 years, mean 71.2; 57% females; 81% white; 19% African-American) in which a complete set of MRI parameters (ICA and CCA) were available. Field sites notified 76 participants for having carotid stenosis of 50% or greater (seven had symptoms of cerebrovascular ischemia; 16 had stenosis above 90%).

Of the 61 participants with a repeat MRI scan, 52 had acceptable carotid wall images for plaque component delineation at both visits. The median interval between replicate scans was 55 days, and between repeated readings of the same scan, 129 days. The MRI technologist acquired BBMRI images in the replicate scan on the side opposite that targeted in the corresponding baseline scan in six cases.

The variables presented herein constitute a selection of available measurements that encompasses the plaque features most relevant to the primary study objectives. The MRI variable definitions and their reliability estimates for quantitative variables are shown in Table 1. Analyses based on small numbers of intrareader and interreader repeat measurements showed little difference in reliabilities, indicating that errors were not primarily due to differences between readers, so both sets of pairs were combined in our estimates of reader reliability. Repeated readings are shown graphically for thickness measurements in Fig. 3 and for area measurements in Fig. 4. Consistent scales were used for linear measurements for both large and small structures. This graphical technique is deliberate, intended to demonstrate the similarity of the magnitude of error measurements for large and small structures and illustrate the reason for the better reliability statistics for the larger structures. Lines of identity were included in these figures to allow easier visualization of any bias. Figure 3 shows no significant bias between linear measurements, with greater differences between repeated measurements for lower values. Figure 4 shows no significant bias and a relatively constant mean difference between measurements across all values.

For linear measurements, our reliability estimates based on repeated MRI scans were 0.77 for MAXIMUM WALL THICKNESS ICA, 0.83 for MAXIMUM WALL THICKNESS FD, 0.89 for MAXIMUM WALL THICKNESS LCCA, and 0.42 for MAXIMUM WALL THICKNESS RCCA, whereas it was less for smaller structures: 0.38 for MEAN CAP THICKNESS and 0.49 for MEAN MINIMUM CAP THICKNESS. Scan variability includes errors due to the reader and variations in scan acquisition. However, as shown in Table 1, repeat scans were generally as reliable as repeat readings of the same scan. Exceptions occurred and may be attributable to sampling variation, but this general conclusion suggests that overall reliability was primarily related to reader variability, and that the error due to the MRI scan acquisition was small.

The resolution of our images was approximately 0.58 mm, which is nearly as large as the errors observed for linear measurements as shown in Fig. 3. This resolution constraint had the greatest impact on the reliability of measuring smaller structures, e.g., fibrous cap thickness. The average absolute errors for LCCA, RCCA and cap thickness measurements were similar to those for thickness measurements for the ICA and FD but reliability estimates were lower because of the narrower range of values between individuals (Fig. 3).

For area measurements, our reliability estimates based on repeated MRI scans were 0.90 for LUMEN AREA LCCA, 0.94 for LUMEN AREA RCCA, and 0.89 for LUMEN AREA FD, whereas it was 0.66 for MAXIMUM LIPID CORE AREA. The lower value for core can again be attributed to the relatively small size of this structure. Similarly, core volume measurements were less reliable than wall volume measurements.

Definitions and reliability estimates for categorical MRI variables are shown in Table 2. Repeat scan agreement ranged from fair to good (16). These estimates were again similar to those based on repeated readings. Mean values, standard deviations, and interquartile ranges of the MRI derived variables for race and gender are shown in Table 3. Mean values were similar in

the pairs sampled for reliability studies. Frequency distributions for categorical variables overall and for race and gender are shown in Table 4.

Not shown is our reanalysis after excluding those in the lowest 10th percentile for vessel wall SI. SI had little effect on the reliability of wall thickness and volume measurements, but too few replicate exams were available to adequately study cap or core measurements.

DISCUSSION

Our findings suggest that reader variability is the primary factor affecting the reliability of MRI measurements of carotid plaque characteristics, and this error is mostly influenced by the size of the structure being measured relative to the spatial resolution of the scanner. Maximum wall thickness and total wall volume were measured most reliably, whereas cap thickness was measured much less reliably. To our knowledge, this is the largest study of these estimates based on both repeated readings and repeated scans and the first population-based study to report descriptive statistics for plaque characteristics by MRI. Interestingly, despite the low-grade narrowing in our cohort (e.g., highest mean maximum stenosis was 9.6%), plaque features of vulnerability for stroke were not uncommon. For example, in white males, lipid cores and hemorrhage were seen in 34% and 8% of plaques, respectively.

We utilized contrast-enhancement to optimize core delineation and cap measurements based on the preferential enhancement of fibrous tissue by the gadolinium contrast agent (6,7). This enables more reliable characterization (6,7) and improves wall volume and area measurements (9). Takaya et al (17) showed that contrast-enhancement reduces the variability of repeated measurements of lipid core size by the same and different readers of BBMRI images. Only one study other than ours, by Saam et al (18), used contrast-enhanced BBMRI to measure reliability of wall area and volume based on repeated scans; however, their measurement errors were likely underestimated since baseline and repeated scans were read together to match image locations. This might explain their superior reliability estimates for maximum core area. Similar to our study, the authors observed larger errors for core area and volume measurements than for wall measurements.

The reliability of repeated scans depends on exam variability (individual MRI technologist performance, patient positioning, equipment characteristics), and reader variability. Unexpectedly, repeated scans were approximately as reliable as repeated readings for quantitative and categorical variables suggesting exam variability was small. This is because the interpretation of scan repeats includes reader errors as well as scan variability. This can be attributed to the protocol design, which emphasized consistent and standardized slice positioning based on carotid geometry, and the considerable effort placed on MRI technologist training and surveillance. Careful attention was made to ensure an orthogonal orientation to the vessel axis to avoid inaccurate wall thickness estimates from oblique slice angles (19–21). Equipment differences, however, could not be assessed.

The measured component size also affected reliability. Measurement errors for MAXIMUM WALL THICKNESS ICA as seen by deviations from the line of identity were small relative to the range of values (Fig. 3). In contrast, the ranges of values for cap and CCA wall thickness measurements were very narrow and errors were large relative to these ranges. Given our resolution of 0.58 mm, we would not expect any greater reliability. This is also supported by the results of Schar et al (22) who demonstrated greater measurement errors with a resolution of ≤4 pixels across the wall. Touze et al (23) similarly reported poorer reader repeatability for cap assessment compared to larger structures. It is remarkable that, despite our resolution constraint, we still observed moderate reliability for measuring small structures such as the fibrous cap. This may relate to the ability of readers to make reasonably accurate visual

interpolations despite the resolution limitations. Because of the strong dependence of reliability on the scan resolution relative to the structure size, we can expect considerably more reliable measurements of these structures at higher fields (e.g., 3T).

Agreement for categorical variables ranged from fair to good with kappa scores similar to those reported by Touze et al (23). For core presence, Touze et al (23) reported reader κ statistics of 0.69 and 0.58 compared with 0.61 in our study. Our agreement for repeated readings was perfect for hemorrhage but only intrareader variability was tested. Calcification degree showed the least reader agreement, with a κ of 0.44. Differences in agreement for calcification may relate to definitions, with Touze et al (23) using identification on at least one slice whereas our definition was based on degree.

Poor reliability estimates limit the ability to differentiate between subjects with different risk factors or disease states unless the sample size is large. Unfortunately our reliability estimates for fibrous cap thickness were based on only 13 replicate exams and 40 repeated readings.

For mean values based on the entire cohort, there was good agreement between our observations and the results of published data. Takaya et al (24) reported MRI measurements for lumen area (61.2 mm^2) and core area (8.8 mm^2) and Zhang et al (9) reported wall volume over a 2-cm segment (732 mm^3) that were similar to our values (Table 3). There are no published reports of cap thickness measurements by MRI, but a histologic study of 171 nonruptured plaque specimens from patients with symptomatic carotid stenosis revealed that 75% of caps were thicker than 180 μ (25). Our corresponding MRI measurements (Table 3) were higher (270–300 μ), likely because the specimen study was of symptomatic high-grade stenosis unlike our cohort, cap specimens can shrink up to 25%, and because of overestimation by MRI due to resolution constraints (19,22). Our observed hemorrhage prevalence is nearly identical to that reported by Saam et al (26) for carotid plaques causing 1% to 15% stenosis.

In conclusion, our results indicate that the most important factor influencing reliability of MRI measurements of plaque characteristics is reader error, and that measurement variability depends largely on the size of the structure analyzed relative to scanner resolution. High field imaging enables improved resolution, though the effect of altered tissue characteristics (e.g., T1, T2) on measurement reliability remains unclear. Our descriptive statistics are based on large numbers weighted to represent the general population and extend the observations from published reports based on small selected samples and histologic measurements of symptomatic and highly stenotic plaques.

Acknowledgments

The Atherosclerosis Risk in Communities Study is carried out as a collaborative study supported by National Heart, Lung, and Blood Institute contracts N01-HC-55015, N01-HC-55016, N01-HC-55018, N01-HC-55019, N01-HC-55020, N01-HC-55021, and N01-HC-55022. The authors thank the staff and participants of the ARIC study for their important contributions.

Contract grant sponsor: National Heart, Lung, and Blood Institute; Contract grant numbers: N01-HC-55015, N01-HC-55016, N01-HC-55018, N01-HC-55019, N01-HC-55020, N01-HC-55021, N01-HC-55022.

REFERENCES

1. Saam T, Ferguson MS, Yarnykh VL, et al. Quantitative evaluation of carotid plaque composition by in vivo MRI. Arterioscler Thromb Vasc Biol 2005;25:234–239. [PubMed: 15528475]
2. Wasserman BA, Sharrett AR, Lai S, et al. Risk factor associations with the presence of a lipid core in carotid plaque of asymptomatic individuals using high-resolution MRI: the multi-ethnic study of atherosclerosis (MESA). Stroke 2008;39:329–335. [PubMed: 18174475]

3. Toussaint JF, LaMuraglia GM, Southern JF, Fuster V, Kantor HL. Magnetic resonance images lipid, fibrous, calcified, hemorrhagic, and thrombotic components of human atherosclerosis in vivo. Circulation 1996;94:932–938. [PubMed: 8790028]
4. Yuan C, Beach KW, Smith LH Jr, Hatsukami TS. Measurement of atherosclerotic carotid plaque size in vivo using high resolution magnetic resonance imaging. Circulation 1998;98:2666–2671. [PubMed: 9851951]
5. Edelman RR, Chien D, Kim D. Fast selective black blood MR imaging. Radiology 1991;181:655–660. [PubMed: 1947077]
6. Cai J, Hatsukami TS, Ferguson MS, et al. In vivo quantitative measurement of intact fibrous cap and lipid-rich necrotic core size in atherosclerotic carotid plaque: comparison of high-resolution contrast-enhanced magnetic resonance imaging and histology. Circulation 2005;112:3437–3444. [PubMed: 16301346]
7. Wasserman BA, Smith WI, Trout HH 3rd, Cannon RO 3rd, Bala-ban RS, Arai AE. Carotid artery atherosclerosis: in vivo morphologic characterization with gadolinium-enhanced double-oblique MR imaging initial results. Radiology 2002;223:566–573. [PubMed: 11997569]
8. Yuan C, Kerwin WS, Ferguson MS, et al. Contrast-enhanced high resolution MRI for atherosclerotic carotid artery tissue characterization. J Magn Reson Imaging 2002;15:62–67. [PubMed: 11793458]
9. Zhang S, Cai J, Luo Y, et al. Measurement of carotid wall volume and maximum area with contrast-enhanced 3D MR imaging: initial observations. Radiology 2003;228:200–205. [PubMed: 12832583]
10. Wasserman BA, Wityk RJ, Trout HH 3rd, Virmani R. Low-grade carotid stenosis: looking beyond the lumen with MRI. Stroke 2005;36:2504–2513. [PubMed: 16239630]
11. Yarnykh VL, Yuan C. T1-insensitive flow suppression using quadruple inversion-recovery. Magn Reson Med 2002;48:899–905. [PubMed: 12418006]
12. The Atherosclerosis Risk in Communities (ARIC) Study: design and objectives. The ARIC investigators. Am J Epidemiol 1989;129:687–702. [PubMed: 2646917]
13. Chu B, Kampschulte A, Ferguson MS, et al. Hemorrhage in the atherosclerotic carotid plaque: a high-resolution MRI study. Stroke 2004;35:1079–1084. [PubMed: 15060318]
14. North American Symptomatic Carotid Endarterectomy Trial.Methods, patient characteristics, and progress. Stroke 1991;22:711–720. [PubMed: 2057968]
15. Fleiss, J. The design and analysis of clinical experiments. New York, NY: John Wiley & Sons, Inc; 1986. p. 1-28.
16. Fleiss, J. Statistical methods for rates and proportions. 2nd ed.. New York, NY: John Wiley & Sons, Inc; 1981. p. 218
17. Takaya N, Cai J, Ferguson MS, et al. Intra- and interreader reproducibility of magnetic resonance imaging for quantifying the lipid-rich necrotic core is improved with gadolinium contrast enhancement. J Magn Reson Imaging 2006;24:203–210. [PubMed: 16739123]
18. Saam T, Kerwin WS, Chu B, et al. Sample size calculation for clinical trials using magnetic resonance imaging for the quantitative assessment of carotid atherosclerosis. J Cardiovasc Magn Reson 2005;7:799–808. [PubMed: 16353440]
19. Antiga L, Wasserman BA, Steinman DA. On the overestimation of early wall thickening at the carotid bulb by black blood MRI, with implications for coronary and vulnerable plaque imaging. Magn Reson Med 2008;60:1020–1028. [PubMed: 18956420]
20. Balu N, Kerwin WS, Chu B, Liu F, Yuan C. Serial MRI of carotid plaque burden: influence of subject repositioning on measurement precision. Magn Reson Med 2007;57:592–599. [PubMed: 17326176]
21. Sato Y, Tanaka H, Nishii T, et al. Limits on the accuracy of 3-D thickness measurement in magnetic resonance images-effects of voxel anisotropy. IEEE Trans Med Imaging 2003;22:1076–1088. [PubMed: 12956263]
22. Schar M, Kim WY, Stuber M, Boesiger P, Manning WJ, Botnager RM. The impact of spatial resolution and respiratory motion on MR imaging of atherosclerotic plaque. J Magn Reson Imaging 2003;17:538–544. [PubMed: 12720263]
23. Touze E, Toussaint JF, Coste J, et al. Reproducibility of high-resolution MRI for the identification and the quantification of carotid atherosclerotic plaque components: consequences for prognosis studies and therapeutic trials. Stroke 2007;38:1812–1819. [PubMed: 17463311]

24. Takaya N, Yuan C, Chu B, et al. Association between carotid plaque characteristics and subsequent ischemic cerebrovascular events: a prospective assessment with MRI--initial results. Stroke 2006;37:818–823. [PubMed: 16469957]

25. Redgrave JN, Gallagher P, Lovett JK, Rothwell PM. Critical cap thickness and rupture in symptomatic carotid plaques: The Oxford Plaque Study. Stroke 2008;39:1722–1729. [PubMed: 18403733]

26. Saam T, Underhill HR, Chu B, et al. Prevalence of American Heart Association type VI carotid atherosclerotic lesions identified by magnetic resonance imaging for different levels of stenosis as measured by duplex ultrasound. J Am Coll Cardiol 2008;51:1014–1021. [PubMed: 18325441]

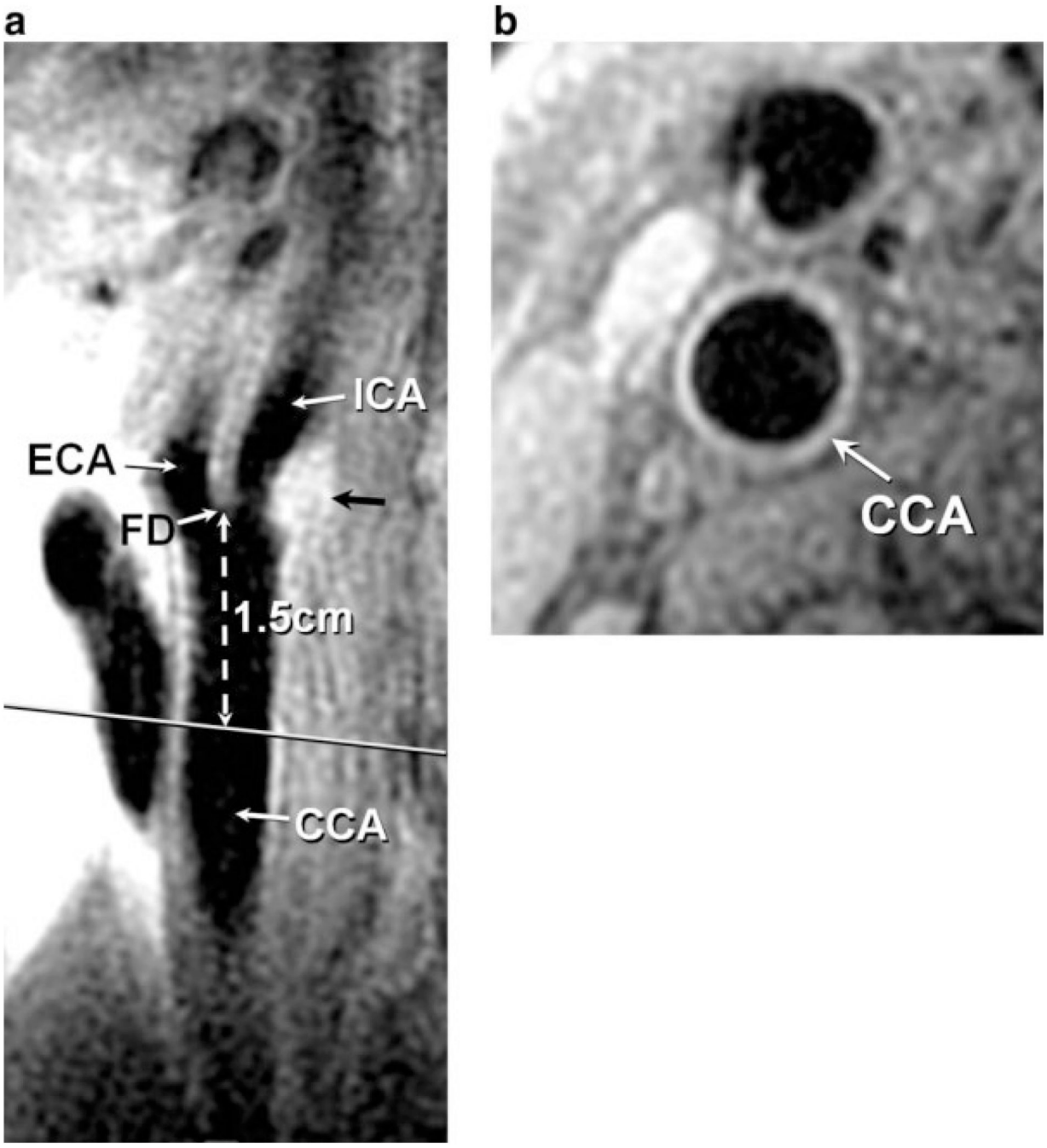

Figure 1.
Slice acquisition through the distal right CCA. A long axis BBMRI image through the carotid bifurcation (**a**) showing the plaque in profile (black arrow) was used to position a T1-weighted BBMRI slice 1.5 cm below the FD (**b**). This was also done on the left side.

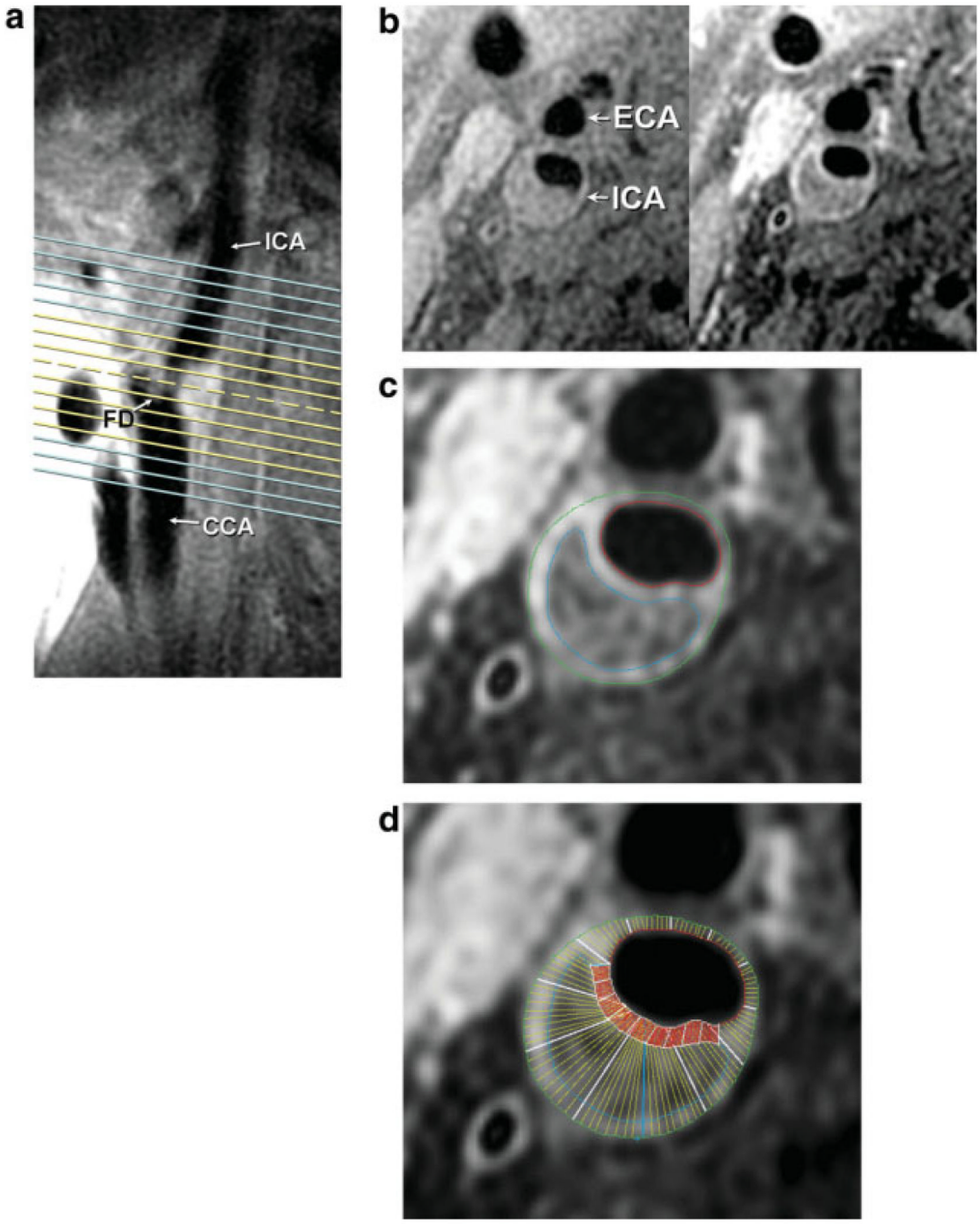

Figure 2.

BBMRI slices through the carotid bifurcation and plaque. A long axis BBMRI image adjacent to the slice shown in Fig. 1a was used to orient eight precontrast (yellow lines) and 16 postcontrast (yellow and blue lines) slices through the plaque. Transverse BBMRI images through the thickest part of the plaque (**a**, broken line) are shown before (left) and after (right) contrast administration (**b**). Contours were drawn on the postcontrast image to delineate the core (blue), lumen (red) and outer wall (green) (**c**). The wall was automatically divided into 12 radial segments and the cap was segmented at 15° increments (**d**). Segmental thickness measurements were determined by averaging the yellow line thicknesses for the wall and red line thicknesses for the cap (d).

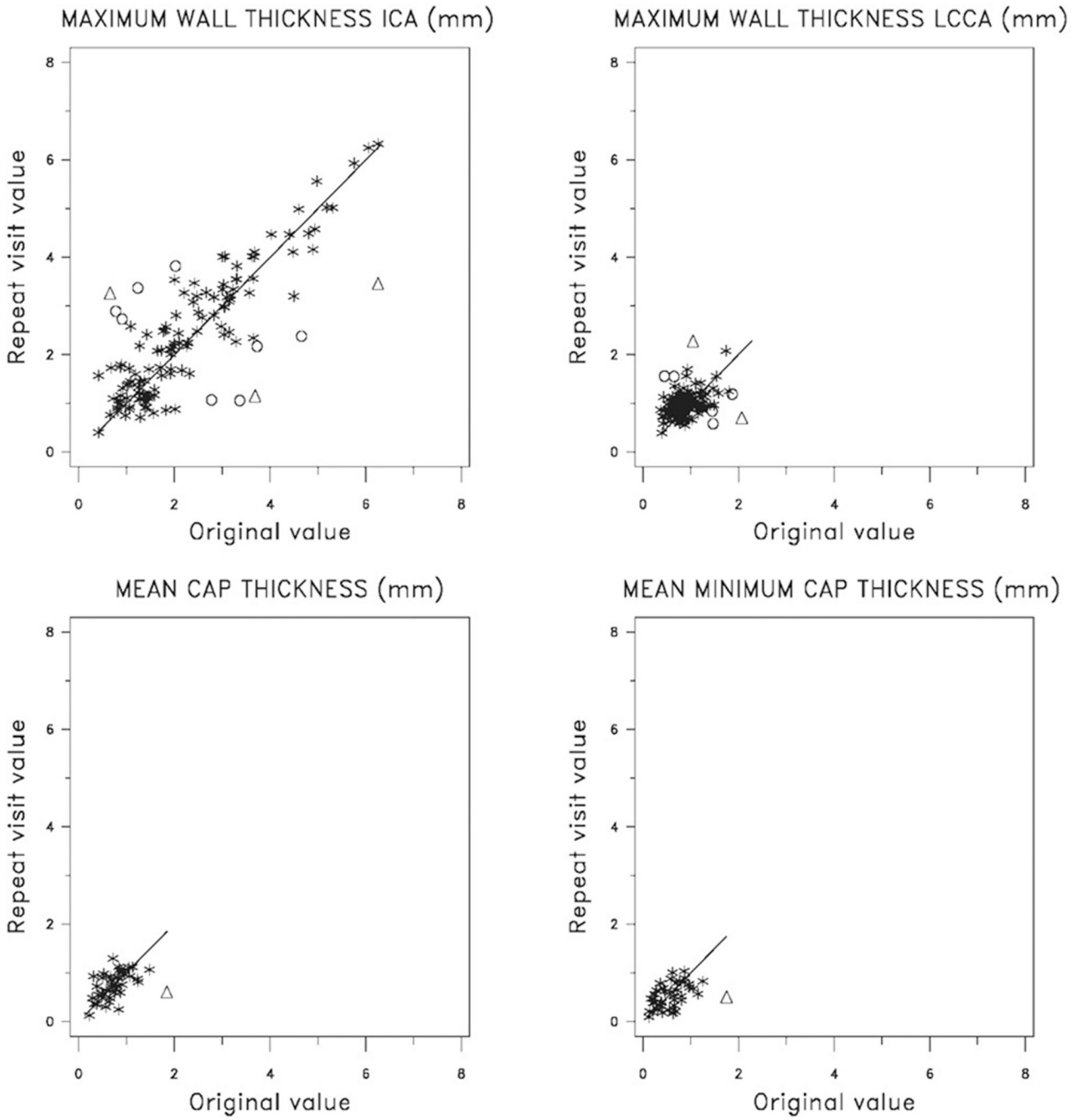

Figure 3.
Reliability of linear measurements based on repeated readings of the same scan. Circles indicate differences larger than 2SD, and triangles larger than 3SD.

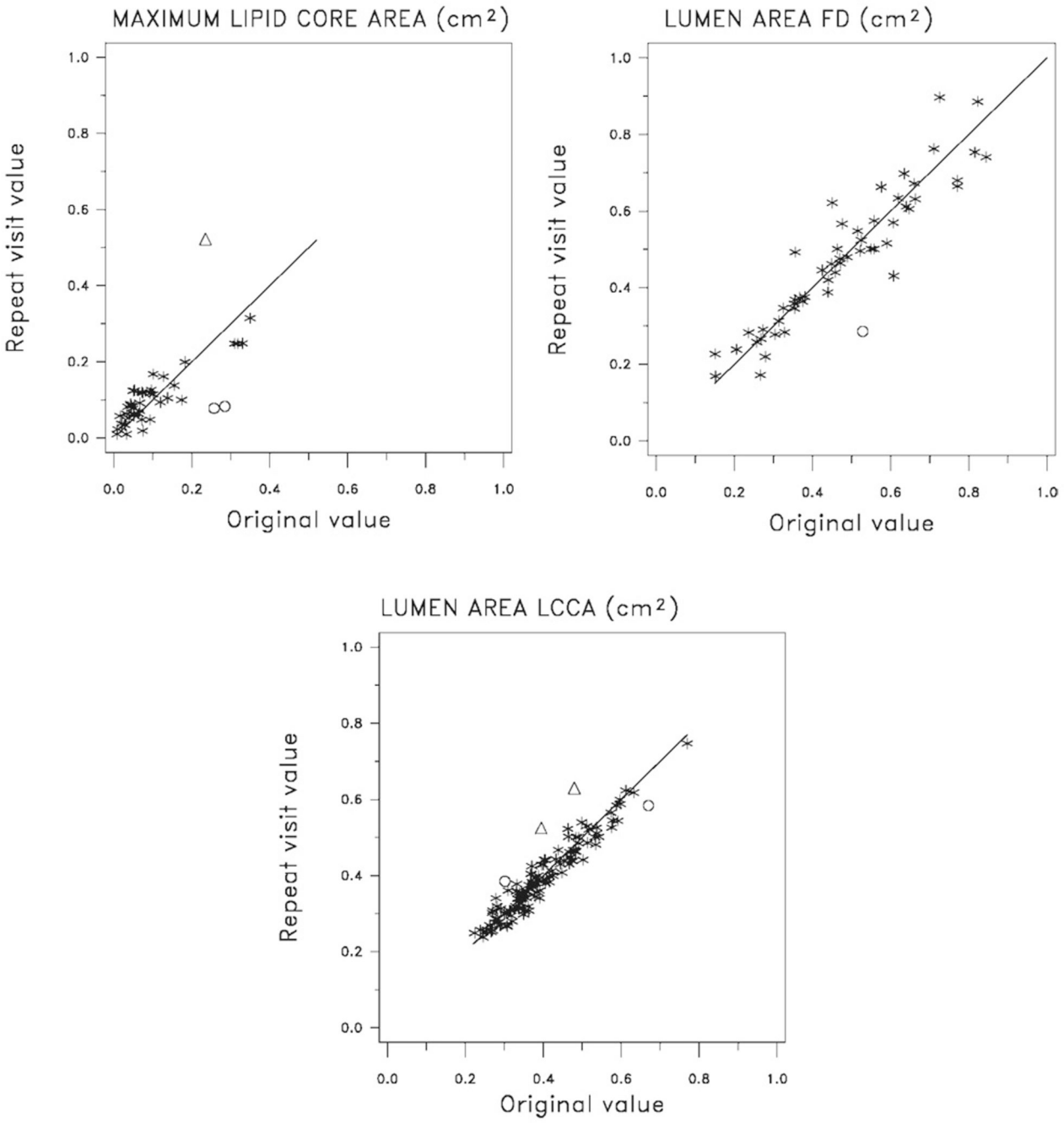

Figure 4.
Reliability of area measurements based on repeated readings of the same scan. Circles indicate differences larger than 2SD, and triangles larger than 3SD.

Table 1

Definitions and Reliability Based on Repeated MRI Scans and Repeated Readings of the Same MRI Scan—Quantitative Variables*

	Repeat Scan				Repeat Reading			
	N	Within person SD	CV	Reliability[a]	*N*	Within person SD	CV	Reliability[a]
TOTAL WALL VOLUME(mL); volume of the ICA wall over eight slices(1.6 cm)	52	0.08	0.17	0.79	130	0.08	0.18	0.76
MAXIMUM WALL THICKNESS ICA (mm); maximum wall thickness of 12 segments at slice with largest core area, or at slice with thickest wall if no core present	49[b]	0.55	0.24	0.77	130	0.57	0.24	0.82
MAXIMUM LIPID CORE AREA (cm^2); maximum core area over eight slices in persons with a core	14	0.05	0.42	0.66	43	0.05	0.45	0.72
TOTAL LIPID CORE VOLUME (ml); total core volume over 8 slices in persons with a core	14	0.06	0.86	0.30	41[c]	0.03	0.48	0.85
MEAN CAP THICKNESS (mm); mean thickness of the cap segments measured at two adjacent slices with largest core	13	0.14	0.18	0.38	40[b]	0.18	0.24	0.60
MEAN MINIMUM CAP THICKNESS (mm); mean of the two minimum cap thicknesses at the two adjacent slices with the largest core	13	0.11	0.22	0.49	40[b]	0.18	0.33	0.59
MAXIMUM WALL THICKNESS LCCA (mm); maximum wall thickness of 12 segments of the left CCA slice	49	0.16	0.15	0.89	127	0.26	0.27	0.24
LUMEN AREA LCCA (cm^2); lumen area of the left CCA slice	50	0.03	0.08	0.90	127	0.02	0.05	0.95
MAXIMUM WALL THICKNESS RCCA (mm); maximum wall thickness of 12 segments of the right CCA slice	50	0.32	0.31	0.42	122[b]	0.22	0.24	0.48

J Magn Reson Imaging. Author manuscript; available in PMC 2010 October 26.

	Repeat Scan				Repeat Reading			
	N	**Within person SD**	**CV**	**Reliability[a]**	***N***	**Within person SD**	**CV**	**Reliability[a]**
LUMEN AREA RCCA (cm^2); lumen area of the right CCA slice	50	0.03	0.07	0.94	125	0.03	0.07	0.91
MAXIMUM WALL THICKNESS FD (mm); maximum wall thickness of 12 segments of the slice 2 mm above the FD	25[b]	0.34	0.22	0.83	54[c]	0.37	0.29	0.77
LUMEN AREA FD (cm^2); lumen area of the slice 2 mm above the FD	26	0.05	0.12	0.89	55[b]	0.05	0.10	0.92
MAXIMUM STENOSIS (%); maximum stenosis on either side	60[b]	7.77	0.95	0.59	157	10.55	0.79	0.66

[*] The ARIC carotid MRI study.

[a] An estimate of the correlation between repeated measurements.

[b] excluding 1 outlier more than 3 SD from mean.

[c] excluding 2 outliers more than 3 SD from mean.

Table 2

Definitions and Reliability Based on Repeated MRI Scans and Repeated Readings of the Same MRI Scan—Categorical Variables

	Repeat scan				Repeat reading			
	N	**Percent agreement**	**Simple kappa**	**SE**	***N***	**Percent agreement**	**Simple kappa**	**SE**
LIPID CORE PRESENCE; presence/absence of core at any of the eight slices	52	73.1	0.45	0.12	130	80.8	0.61	0.07
CALCIUM; maximum calcium area at any of the eight slices: absent, below or above the weighted median value	53	71.7	0.50	0.10	139	70.5	0.44	0.07
HEMORRHAGE; presence/absence intraplaque hemorrhage	59	91.5	0.62	0.16	11	100.0*	—	—

* Based on assessments by one reader.

The ARIC Carotid MRI Study.

SE = standard error.

Table 3

Means, Standard Deviations, and Interquartile Ranges of Quantitative MRI Variables for Race and Gender[†]

	Black males (Mean ± SD, IQR)	Black females (Mean ± SD, IQR)	White males (Mean ± SD, IQR)	White females (Mean ± SD, IQR)	*P* value[*]
Total wall volume (mL)	0.436 ± 0.150	0.359 ± 0.113	0.496 ± 0.189	0.386 ± 0.138	<0.0001
	0.342–0.497	0.292–0.413	0.367–0.565	0.292–0.451	
Maximum wall thickness	1.85 ± 1.07	1.65 ± 0.95	2.32 ± 1.29	1.84 ± 0.96	<0.0001
ICA (mm)	1.06–2.23	0.96–2.01	1.30–3.02	1.08–2.46	
Maximum lipid core	0.09 ± 0.08	0.08 ± 0.08	0.13 ± 0.13	0.09 ± 0.08	<0.01
area (cm^2)	0.04–0.11	0.03–0.12	0.05–0.17	0.04–0.12	
Total lipid core volume (mL)	0.050 ± 0.078	0.040 ± 0.043	0.080 ± 0.099	0.050 ± 0.060	<0.01
	0.014–0.055	0.008–0.053	0.022–0.111	0.013–0.069	
Mean cap thickness (mm)	0.66 ± 0.27	0.65 ± 0.29	0.70 ± 0.31	0.64 ± 0.28	0.47
	0.42–0.80	0.45–0.83	0.48–0.88	0.44–0.83	
Mean minimum cap	0.48 ± 0.21	0.47 ± 0.25	0.49 ± 0.25	0.47 ± 0.25	0.87
thickness (mm)	0.30–0.62	0.29–0.62	0.29–0.68	0.27–0.67	
Maximum wall thickness	0.92 ± 0.26	0.84 ± 0.23	1.02 ± 0.38	0.94 ± 0.25	<0.0001
LCCA (mm)	0.76–1.04	0.68–0.91	0.82–1.12	0.78–1.06	
Lumen area LCCA (cm^2)	0.44 ± 0.11	0.39 ± 0.09	0.41 ± 0.10	0.34 ± 0.08	<0.0001
	0.37–0.48	0.33–0.44	0.34–0.46	0.29–0.39	
Maximum wall thickness	0.87 ± 0.20	0.84 ± 0.21	0.98 ± 0.31	0.95 ± 0.30	<0.0001
RCCA (mm)	0.75–0.97	0.70–0.96	0.80–1.07	0.77–1.04	
Lumen area RCCA (cm^2)	0.46 ± 0.12	0.40 ± 0.09	0.42 ± 0.11	0.35 ± 0.08	<0.0001
	0.38–0.51	0.34–0.44	0.34–0.49	0.30–0.40	
Maximum wall thickness	1.32 ± 0.82	1.06 ± 0.55	1.68 ± 1.10	1.31 ± 0.74	<0.0001
FD (mm)	0.85–1.38	0.78–1.04	0.95–2.05	0.87–1.40	
Lumen area FD (cm^2)	0.57 ± 0.20	0.49 ± 0.19	0.47 ± 0.19	0.39 ± 0.14	<0.0001
	0.41–0.74	0.37–0.58	0.34–0.58	0.29–0.46	
Maximum stenosis (%)	6.32 ± 12.67	6.46 ± 13.17	9.61 ± 16.82	7.00 ± 12.79	0.0023
	0.00–7.00	0.00–10.0	0.00–14.0	0.00–10.0	

[†]Based on a study population of 1769 participants. All values were weighted to represent the entire ARIC cohort.

* *P* values represent the difference among the four mean values by ANOVA.

IQR = interquartile range.

Table 4

Frequencies of Categorical Variables for Race and Gender[†]

	Overall ***N*** **(%)**	**Black males** ***N*** **(%)**	**Black females** ***N*** **(%)**	**White males** ***N*** **(%)**	**White females** ***N*** **(%)**	***P*-value**[*]
Lipid core presence	573 (26.5)	44 (21.2)	54 (23.6)	282 (34.0)	193 (21.9)	0.0002
Calcium area ≥ weighted mean value	308 (11.1)	25 (10.8)	24 (7.0)	177 (17.5)	82 (7.1)	<0.0001
Hemorrhage	118 (4.1)	4 (2.0)	6 (1.5)	83 (8.0)	25 (1.9)	<0.0001

[†]AII percentages were weighted to represent the entire ARIC cohort.

[*]*P* values represent the difference among four proportions by Rao-Scott chi-square analysis.